J|A|C|S COMMUNICATIONS

Published on Web 11/13/2009

Direct Synthesis of Cubic $ZrMo_2O_8$ Followed by Ultrafast In Situ Powder Diffraction

Jennifer E. Readman,[†] Sarah E. Lister,[†] Lars Peters,[‡] Jon Wright,[§] and John S. O. Evans*[,†]

Department of Chemistry, Durham University, Durham DH1 3LE, United Kingdom, Christian-Albrechts-Universität zu Kiel, Institut für Geowissenschaften, Kiel, Germany, and European Synchrotron Radiation Facility, Grenoble, France

Received September 9, 2009; E-mail: john.evans@durham.ac.uk

There has been a considerable amount of interest in negative thermal expansion (NTE) phases which are of importance, for example, in the manufacture of low or zero expansion composite materials. The cubic AM_2O_8 family of materials are of particular interest as the magnitude and isotropic nature of the NTE give them great technological potential.[1−3] The exemplar material, cubic ZrW_2O_8, has been widely studied and can be prepared by a variety of methods including high temperature synthesis from the component oxides at 1473 K followed by rapid quenching. Once this metastable phase is formed it is kinetically stable up to ∼1050 K. There are two potential disadvantages of using ZrW_2O_8 in composite materials. First, it undergoes a phase transition from the α to β form which, although both phases show strong NTE, causes a discontinuity in the lattice parameters at ∼450 K.[4,5] Second, a pressure of 0.21 GPa induces a cubic to orthorhombic phase transition resulting in a denser structure with an ∼5% lower volume and a less negative (or positive) coefficient of NTE which may be detrimental in applications.[5]

In contrast, the cubic form of $ZrMo_2O_8$ (γ-$ZrMo_2O_8$ [6]) does not show any major discontinuities in lattice parameter with temperature and pressure induced transitions are reversible at room temperature,[7,8] making it more attractive for composite materials. Unlike cubic ZrW_2O_8, it has not been possible to synthesize γ-$ZrMo_2O_8$ directly from the constituent oxides, and the cubic phase has been assumed to be thermodynamically metastable at all temperatures.[9] Synthesis at temperatures above 670 K gives the trigonal phase (α-$ZrMo_2O_8$),[10−12] while at lower temperatures the thermodynamically stable phase is monoclinic β-$ZrMo_2O_8$.[11,13] The enthalpies of formation of some AM_2O_8 phases from the binary oxides were investigated by Varga et al.[9] They found the enthalpy of formation becomes more endothermic from β-$ZrMo_2O_8$ → α-$ZrMo_2O_8$ → γ-$ZrMo_2O_8$ → amorphous $ZrMo_2O_8$ and that the monoclinic β-$ZrMo_2O_8$ phase is the only enthalpically stable phase at room temperature. Preparation of $ZrMo_2O_8$ phases is further complicated by the volatility of MoO_3, and trigonal $ZrMo_2O_8$ has been shown to lose MoO_3 above ∼1125 K.[14]

The recognized synthetic procedure for the formation of γ-$ZrMo_2O_8$ involves the careful decomposition of a hydrated precursor phase, $ZrMo_2O_7(OH)_2 \cdot 2H_2O$, via another polymorph LT-$ZrMo_2O_8$.[7,8,15] Work by Lind et al. highlighted that the precise reagents used in the synthesis of this precursor can significantly alter the ratios of γ-$ZrMo_2O_8$ and α-$ZrMo_2O_8$ formed upon dehydration, with the cubic γ-phase only being accessible in a very narrow temperature window.[7,8]

Surprisingly we recently obtained indications that it may be possible to form the supposedly metastable cubic phase by firing the constituent oxides at high temperatures (∼1450 K) for a few seconds followed by very rapid quenching. These conditions differ markedly from the careful kinetic control used in previous synthetic routes but proved hard to investigate in a conventional manner due to the extremely short time scales over which different phases appeared. In this communication we show that rapid in-situ powder X-ray diffraction experiments prove unambiguously that supposedly metastable cubic γ-$ZrMo_2O_8$ can be synthesized directly from the oxides. Full quantitative analysis of the reacting systems and observation of transient intermediates on time scales down to 0.1 s give significant insight into the process.

All in-situ experiments were carried out at beamline ID11 at the European Synchrotron Radiation Facility (ESRF) using a wavelength of 0.19902(2) Å. Stoichiometric amounts of ZrO_2 and MoO_3 were mixed and packed into 0.57 mm diameter Pt capillaries with a 0.04 mm wall thickness, and the ends mechanically sealed. A Frelon 2K CCD 2D detector[16] was used at a minimum readout time of 20 ms and allowed collection of diffraction patterns of sufficient quality for quantitative Rietveld refinement in as little as 0.1 s. A mirror furnace was used to rapidly generate the high temperatures required for synthesis.[17] The furnace was constructed from a ceramic body with three halogen lamps as the heat source. The temperature was controlled by the amount of power to the bulbs; quoted here as a simple % of maximum power. An approximate calibration of temperature versus heater power was carried out prior to data collection based on the thermal expansion of Al_2O_3 and the Pt of the capillary.[18] In a typical experiment, the capillary containing the reaction mixture was translated into the preheated furnace and data were collected in 0.25 s time slices for 120 s (480 separate patterns) before the furnace power was turned off and the sample was allowed to cool. Samples typically reached ∼1400 K within 5 s and cooled by 500 K within a similar period. Fit2D was used to integrate raw diffraction images,[19] and Powder3D[20] was used to generate 2D surface plots of the data to allow quick qualitative examination.

For quantitative analysis, Rietveld refinements were carried out using the program TOPAS.[21] Five phases were included in all refinements, MoO_3,[22] ZrO_2,[23] α-$ZrMo_2O_8$,[9,10] γ-$ZrMo_2O_8$,[7] and Pt[24] from the capillary. An 18 term background function together with a pseudo-Voigt peak profile function was used. All lattice parameters were allowed to vary, but individual atomic coordinates were not. An overall isotropic thermal parameter was included for all phases except Pt, for which a separate isotropic thermal parameter was used.[25] The localized nature of the "hot spot" in the mirror furnace means that it is not possible to measure the variation in sample temperature throughout the experiment using a thermocouple. Temperature was therefore estimated based on refined cell parameters of the Pt capillary using an expression derived from thermal expansion coefficients reported by Edwards et al. and Manoun et al.[26−28] An independent check was performed using thermal expansion data for ZrO_2,[29] with little difference between

[†] University of Durham.
[‡] Christian-Albrechts-Universität zu Kiel.
[§] European Synchrotron Radiation Facility.

10.1021/ja907648z

the two methods. The resulting temperature profiles for all experiments are given in the Supporting Information.

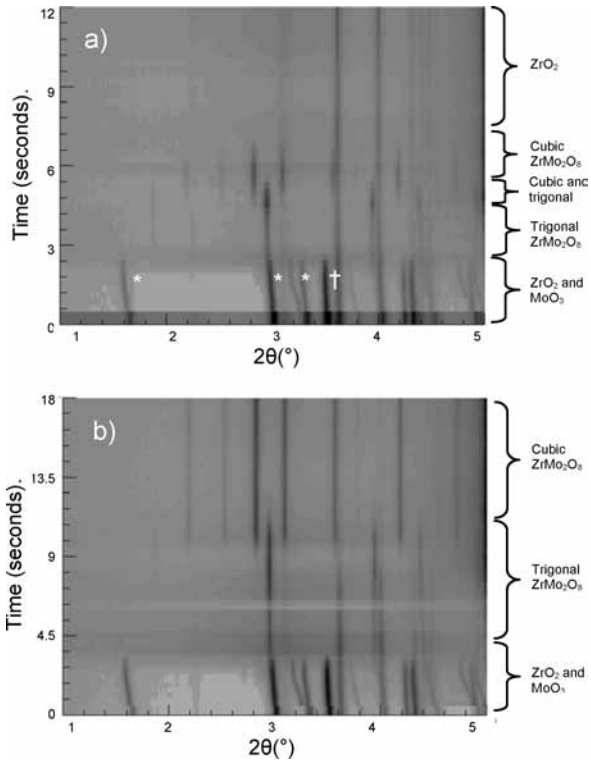

Figure 1. Two-dimensional film plots of the diffraction data obtained for (a) ratio of ZrO_2 and MoO_3 1:2 in the starting mixture at 1520 K and (b) ratio of ZrO_2 and MoO_3 1:3 in the starting mixture at 1400 K. The strongest ZrO_2 and MoO_3 peaks are indicated by † and * respectively.

Figure 1a shows diffraction data obtained using a furnace power of 72%. We estimate that this corresponds to a temperature after 100 s in the furnace, T_{100}, of 1520 K. At low temperature, diffraction peaks correspond to ZrO_2, MoO_3, and the Pt of capillary walls as expected. On inserting the sample into the furnace, all peaks initially shift to lower 2θ indicating positive thermal expansion; certain reflections of MoO_3 shift more dramatically due to marked anisotropy in the thermal expansion of this layered structure. Between approximately 1.6 and 2.5 s ($T \approx 1030$ and 1260 K) peaks due to MoO_3 disappear and those of trigonal α-$ZrMo_2O_8$ are observed for the first time. A drop in the overall diffracted intensity occurs at this point, which is consistent with the melting of MoO_3 ($T_{melt} = 1068$ K).[9] Between 2.5 and 5 s ($T \approx 1434$ K) the amount of trigonal α-$ZrMo_2O_8$ increases before gradually disappearing. New peaks corresponding to cubic γ-$ZrMo_2O_8$ appear from 4.5 s ($T \approx 1400$ K). These peaks disappear after a total elapsed time of 8 s ($T \approx 1525$ K), and ZrO_2 is the only crystalline material that remains. On quenching after 120 s (T falls from ~1520 to ~700 K within 8 s), significant quantities of cubic $ZrMo_2O_8$ were again observed in the diffraction data.

Results from the quantitative phase analysis are shown in Figure 2a. The data are plotted as Rietveld scale factor × number of formula units per unit cell × molar mass × volume, or *ZMV*. This allows for absolute comparison between the different phases. We note that *ZMV* values derived before heating are consistent with a 1:2 molar ratio of ZrO_2 to MoO_3 as expected. Quantitative analyses confirm the phase evolution and show that cubic γ-$ZrMo_2O_8$ can be formed directly from the oxides but is only stable for a few seconds under these conditions.

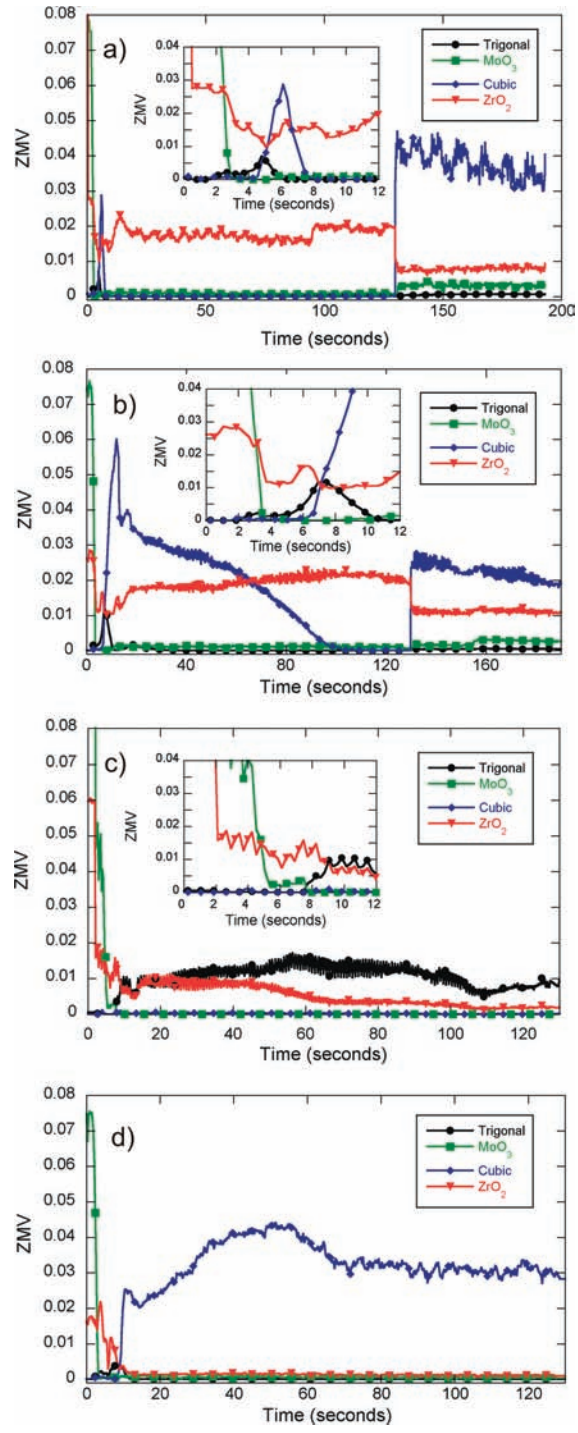

Figure 2. Plots of composition obtained by quantitative Rietveld refinement versus time for experiments discussed. (a) ZrO_2/MoO_3 1:2 in starting mixture and 72% heater power ($T_{100} = 1520$ K), (b) ZrO_2, MoO_3 1:2 in starting mixture and 70% heater power ($T_{100} = 1470$ K), (c) ZrO_2/MoO_3 1:2 in starting mixture and 68% heater power ($T_{100} = 1350$ K), and (d) ZrO_2: MoO_3 1:3 in starting mixture and 70% heater power ($T_{100} = 1400$ K).

The observation that cubic γ-$ZrMo_2O_8$ disappeared during heating in this experiment, yet reformed on cooling, suggested that a lower temperature might favor the formation of crystalline cubic γ-$ZrMo_2O_8$. The experiment was therefore repeated at a lower power of 70% which corresponds to a final temperature of $T_{100} \approx 1470$ K. Under these conditions melting of MoO_3 was again observed from ~1060 K, followed by growth of the trigonal phase which reached maximum intensity at ~7 s (Figure 2b). Significant

amounts of the cubic phase began to form from ~6.5 s ($T \approx 1350$ K), and it was the dominant crystalline material with maximum intensity after ~12 s ($T \approx 1360$ K). After this point there was a slow increase in sample temperature (reaching ~1460 K by the end of the heating period), and *ZMV* of the cubic phase steadily decreased to zero. This loss of γ-$ZrMo_2O_8$ was accompanied by only a small rise in *ZMV* for ZrO_2. Again, once the heater was switched off, we observed γ-$ZrMo_2O_8$ on cooling. There was no evidence for the formation of the trigonal phase during this latter stage of the experiment. The loss of γ-$ZrMo_2O_8$ is consistent with either volatilization of MoO_3 (though one might then expect a more significant rise in *ZMV* of ZrO_2) or melting of γ-$ZrMo_2O_8$. We note that the phase diagram of ZrO_2-WO_3 has a peritectic point at 1530 K such that cubic ZrW_2O_8 melts to form ZrO_2 and a liquid slightly richer in WO_3.[30]

Decreasing the power to the heater to 68% ($T_{100} \approx 1350$ K) results in trigonal α-$ZrMo_2O_8$ being formed after 8 s ($T \approx 1350$ K), persisting over the course of the entire experiment, even upon cooling, Figure 2c. There is no evidence of γ-$ZrMo_2O_8$ being formed at any time during the experiment. We conclude that this temperature is too low for formation of the cubic phase.

These three experiments were carried out using a ratio of 1:2 ZrO_2/MoO_3, and it is notable that ZrO_2 is observed throughout the experiments. It is well known, however, that MoO_3 is volatile at high temperatures, which suggests that MoO_3 could be lost from the hot zone of the capillary at the temperatures used before it can react. A further experiment was therefore carried out using a ZrO_2/MoO_3 ratio of 1:3 at a power of 70%, the results of which are shown in Figures 1b and 2d. Under these conditions trigonal $ZrMo_2O_8$ forms from ~4 s (T ~1310 K) and transforms cleanly to cubic γ-$ZrMo_2O_8$ from ~8 s (T ~1400 K), which is the only crystalline phase present thereafter.

These experiments show conclusively, and for the first time, that cubic γ-$ZrMo_2O_8$ can be synthesized directly from its constituent oxides, in contrast to previous assumptions. The reaction proceeds extremely rapidly at elevated temperatures with formation occurring within seconds at ~1360−1400 K. Reactions appear to occur via initial melting of MoO_3 which is accompanied by formation of trigonal $ZrMo_2O_8$. This phase grows in intensity, typically peaking around the point where the cubic phase starts to form. We note that similar experiments on ZrW_2O_8 in which the capillary temperature was gradually increased showed formation over a much slower (~60 min) time scale at a temperature estimated from the Pt cell parameter of ~1359 K. The published phase diagram shows ZrW_2O_8[30] is stable above 1378 K which gives confidence in our estimated sample temperatures. Cubic γ-$ZrMo_2O_8$ is stable over the time periods of these experiments at a temperature of ~1400 K, as evidenced by the data of Figure 2d. The data of Figure 2a and 2b both show that as temperature exceeds ~1460 K the amount of crystalline γ-$ZrMo_2O_8$ decreases significantly. These observations are consistent with melting at this temperature. These preliminary investigations suggest that the high temperature behavior of $ZrMo_2O_8$ is not dissimilar to that of ZrW_2O_8, which is thermodynamically stable from 1378 to 1530 K. The cubic phases of both materials are presumably entropically stabilized at high temperature.

Acknowledgment. We would like to thank EPSRC for sponsorship under Grant EP/C538927/1 and STFC for access to facilities at the ESRF. S.E.L. thanks Durham University for a Doctoral Training Fellowship.

Supporting Information Available: 2D film plots for the experiments not shown are available as Supporting Information along with temperature profiles for all experiments. This material is available free of charge via the Internet at http://pubs.acs.org.

References

(1) Evans, J. S. O. *J. Chem. Soc., Dalton Trans.* **1999**, 3317.
(2) Sleight, A. W. *Annu. Rev. Mater. Sci.* **1998**, *28*, 29.
(3) Sleight, A. W. *Inorg. Chem.* **1998**, *37*, 2854.
(4) Mary, T. A.; Evans, J. S. O.; Vogt, T.; Sleight, A. W. *Science* **1996**, *272*, 90.
(5) (a) Evans, J. S. O.; Mary, T. A.; Vogt, T.; Subramanian, M. A.; Sleight, A. W. *Chem. Mater.* **1996**, *8*, 2809. (b) Evans, J. S. O.; Hu, Z.; Jorgensen, J. D.; Argyriou, D. N.; Short, S.; Sleight, A. W. *Science* **1997**, *275*, 61.
(6) We note that the nomenclature of $ZrMo_2O_8$ phases is, confusingly, different from that of ZrW_2O_8 but follows here normal conventions in the literature.
(7) Lind, C.; Wilkinson, A. P.; Hu, Z.; Short, S.; Jorgensen, J. D. *Chem. Mater.* **1998**, *10*, 2335.
(8) Lind, C.; Wilkinson, A. P.; Rawn, C. J.; Payzant, E. A. *J. Mater. Chem.* **2001**, *11*, 3354.
(9) Auray, M.; Quarton, M.; Tarte, P. *Acta Crystallogr.* **1986**, *C42*, 257.
(10) Auray, M.; Quarton, M.; Tarte, P. *Powder Diffraction* **1987**, *2*, 36.
(11) Serezhkin, V. N.; Efremov, V. A.; Trunov, V. K. *Russ. J. Inorg. Chem.* **1987**, *32*, 1568.
(12) Klevtsova, R. F.; Glinskaya, L. A.; Zolotova, E. S.; Klevtsov, P. V. *Doklady Akademii Nauk SSSR* **1989**, *305*, 91.
(13) Varga, T.; Lind, C.; Wilkinson, A. P.; Xu, H.; Lesher, C. E.; Navrotsky, A. *Chem. Mater.* **2007**, *19*, 468.
(14) Samant, M. S.; Dharwadkar, S. R.; Phadnis, A B.; Namboodiri, P. N. *Mater. Chem. Phys.* **1993**, *35*, 120.
(15) Allen, S.; Warmingham, N. R.; Gover, R. K. B.; Evans, J. S. O. *Chem. Mater.* **2003**, *15*, 3406.
(16) Labiche, J. C.; Mathon, O.; Pascarelli, S.; Newton, M. A.; Ferre, G. G.; Curfs, C.; Vaughan, G.; Homs, A.; Carreiras, D. F. *Rev. Sci. Instrum.* **2007**, *78*, 091301.
(17) Moussa, S. M.; Ibberson, R. M.; Bieringer, M.; Fitch, A. N.; Rosseinsky, M. J. *Chem. Mater.* **2003**, *15*, 2527.
(18) Stinton, G. W.; Evans, J. S. O. *J. Appl. Crystallogr.* **2007**, *40*, 87.
(19) Hammersley, A. P.; Svensson, S. O.; Hanfland, M.; Fitch, A. N.; Häusermann, D. *High Pressure Res.* **1996**, *14*, 235.
(20) Hinrichsen, B.; Dinnebier, R. E.; Jansen, M. *Z. Kristallogr.* **2004**, *23*, 231.
(21) A.A. Coelho, TOPAS v4.1: General Profile and Structure Analysis Software for Powder Diffraction Data, 2008.
(22) Kihlborg, L. *Ark. Kemi* **1963**, *21*, 357.
(23) Hill, R. J.; Cranswick, L. M. D. *J. Appl. Crystallogr.* **1994**, *27*, 802.
(24) Swanson, H. E.; Tatge, E. *Natl. Bur. Stand.* **1953**, *539*, 1.
(25) Pt of the capillaries initially shows significant texture effects due to the manufacturing process. Diffracted intensities therefore change through the experiment as Pt recrystallizes. This does not affect cell parameter determination significantly.
(26) From the thermal expansion data a polynomial was derived from which the temperature could be calculated from the refined Pt lattice parameter. The polynomial is of the form $\text{Temp(K)} = (((-1.90601 \times 10^{-5}) - (4.64016 \times 10^{-8}) \times (3.91704 - \text{lpa}))^{0.5})/(2.231 \times 10^{-8})$, where lpa is the refined Pt lattice parameter at that particular temperature.
(27) Edwards, J. W.; Speiser, R.; Johnston, H. L. *J. Appl. Phys.* **1951**, *22*, 424.
(28) Manoun, B.; Saxena, S. K.; Liermann, H. P.; Barsoum, M. W. *J. Am. Ceram. Soc.* **2005**, *88*, 3489.
(29) Taylor, D. *Br. Ceram. Trans. J.* **1985**, *84*, 9.
(30) Chang, L. L. Y.; Scroger, M. G.; Phillips, B. *J. Am. Ceram. Soc.* **1967**, *50*, 211.

JA907648Z